CONTEMPORARY MATHEMATICS

628

Biological Fluid Dynamics: Modeling, Computations, and Applications

AMS Special Session
Biological Fluid Dynamics: Modeling, Computations, and Applications
October 13, 2012
Tulane University, New Orleans, Louisiana

Anita T. Layton
Sarah D. Olson
Editors

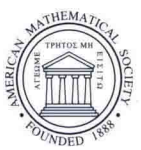

American Mathematical Society

CONTEMPORARY MATHEMATICS

628

Biological Fluid Dynamics: Modeling, Computations, and Applications

AMS Special Session
Biological Fluid Dynamics: Modeling, Computations, and Applications
October 13, 2012
Tulane University, New Orleans, Louisiana

Anita T. Layton
Sarah D. Olson
Editors

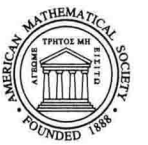

American Mathematical Society
Providence, Rhode Island

2010 *Mathematics Subject Classification.* Primary 76M25, 76Z05, 74F10, 35Q92, 92C35, 92B05, 92C05, 92C10, 62P10.

Library of Congress Cataloging-in-Publication Data

Biological fluid dynamics: modeling, computation, and applications: AMS Special Session on Biological Fluid Dynamics: Modeling, Computation, and Applications: October 13, 2012, Tulane University, New Orleans, Louisiana / Anita T. Layton, Sarah D. Olson, editors.
pages cm. – (Contemporary mathematics ; volume 628)
Includes bibliographical references.
ISBN 978-0-8218-9850-5 (alk. paper)
1. Hemodynamics–Congresses. 2. Rheology (Biology)–Congresses. 3. Body fluid flow–Congresses. 4. Fluid dynamics–Congresses. I. Layton, Anita T., 1973- editor of compilation. II. Olson, Sarah D., 1981- editor of compilation.

QP105.7.B54 2014
612′.01522–dc23 2014011913

Contemporary Mathematics ISSN: 0271-4132 (print); ISSN: 1098-3627 (online)

DOI: http://dx.doi.org/10.1090/conm/628

Biological Fluid Dynamics: Modeling, Computations, and Applications

Preface

This volume is a result of a special session at the AMS Fall Southeastern Sectional Meeting, which was held at Tulane University in New Orleans, LA, October, 2012. That special session was focused on simulating the motion of an incompressible fluid driven by flexible immersed structures. Active biological tissue is typically constructed of fibers that are surrounded by fluid; the fibers not only hold the tissue together but also transmit forces that ultimately result in fluid motion. In other cases, the fluid may flow through flexible conduits such as blood vessels or airways that both react to and affect the fluid dynamics. Additional examples arise in the context of external fluid flows in biological and engineering applications, such as the dynamics of insect wings, flagellated or ciliated organisms, suspensions of blood cells and other synthetic particles. In addition to solving biologically motivated questions, there is tremendous interest in the development and application of advanced computational techniques to solve these fluid-structure interaction problems.

Given the widespread interest among mathematicians, biologists, and engineers in fluid-structure interaction problems, we believe that this volume is both timely and valuable; this is particularly true because of recent algorithmic improvements. The focus of this volume will be on three main themes: (i) formulation and analysis of mathematical equations that describe fluid-structure interactions in biological systems, (ii) algorithmic and computational issues related to increasing accuracy and efficiency through use of adaptivity, time-stepping scheme, and regularization, and (iii) applications to problems in biological and physical sciences, and interpretation of model results.

This volume is organized as follows. It begins with two review articles that discuss the numerical and computational aspects of fluid-structure interaction problems. Specifically, these articles focus on the mathematical equations describing the fluid and structure, as well they describe state of the art computational approaches to solve the coupled system of equations. Next are original articles that study small-scale fluid motion driven by cilia and flagella. Biological questions are addressed in terms of transport of fluid as well as the development and extension of new numerical methods. Also included are articles that consider a wide variety of physiological examples, including peristalsis, platelet adhesion and cohesion, upside-down jellyfish, and dynamics in the rat kidney.

Contents

Contemporary Mathematics
Volume **628**, 2014
http://dx.doi.org/10.1090/conm/628/12545

Simulating Biofluid-Structure Interactions with an Immersed Boundary Framework – A Review

Sarah D. Olson and Anita T. Layton

ABSTRACT. This review focuses on biofluid-structure interactions that are modeled using an immersed boundary framework. We consider elastic structures immersed in a viscous, incompressible fluid that interact with the fluid via a forcing term in the momentum equation. The standard immersed boundary (IB) method of Peskin is reviewed in terms of numerical implementation, force derivation, and choice of compactly supported delta function. We then review related methods including the immersed interface method, generalized IB method, and regularized Stokeslets methods. Several advances in numerical methods are detailed, including porous boundaries, multi-fluids, time stepping strategies, and the incorporation of viscoelasticity. The review ends with a discussion of advantages of several methods and avenues of future research.

1. Introduction

The interaction between fluid flows and immersed structures are nonlinear multi-physics phenomena, and their applications can be found in a wide range of scientific and engineering disciplines. In biology, many applications can be found, including dynamics of insect wings, flagellated or ciliated organisms, suspensions of blood cells and other synthetic particles, parachute dynamics, and many more. This is an active area of research in terms of development of new numerical methods as well as model development for the structure.

The IB method was originally developed by Peskin [**137**, **138**], for studying blood flow through a beating heart [**134**]. In this method, a dynamic elastic structure is immersed in a viscous, incompressible fluid. This mathematical formulation and numerical method is a framework to model fluid-structure interaction problems by mechanically coupling the fluid to forces in a support region around the structure. This is a fully coupled system since the structure is able to alter the fluid velocity via time and spatially dependent forces exerted on the surrounding fluid, and in turn, the movement of the structure is determined by the local fluid velocity.

We will keep with the theme of this volume and focus on aspects of the IB method of Peskin (1972) and related methods to model biological elastic structures interacting with a fluid. Since the initial development of the IB method, several different extensions and variations have been developed. This review will focus on

2010 *Mathematics Subject Classification.* Primary 76M25, 76Z05, 76Z05.
NSF DMS 1122461.

related methods including the immersed interface method, a sharp interface method with potentially higher order accuracy, and the method of regularized Stokeslets for zero Reynolds number applications. We refer the interested reader to reviews on IB methods for solids [**121**], engineering applications of fluid-structure interaction [**44**, **122**], and numerical methods for fluid-structure interaction [**20**, **71**].

In this review, we will focus on the IB method, its applications, and additional extensions. A general overview of the IB method and its implementation will be detailed in §2.1, and applications will be discussed in §4. The IB method has also motivated the development of the immersed interface method and the method of regularized Stokeslets, which will be detailed in §2.2 and §2.3 . A few recent advances for modeling biological structures, e.g. porous boundaries and multi-fluid domains, will also be highlighted in §3. We will end this review with a discussion of advantages of particular methods and future avenues of research.

2. Numerical formulations

2.1. Immersed boundary (IB) method. This is a non-conforming method as two different grids will be used for the structure and the fluid. The fluid motion will be described by a set of Eulerian variables defined on a Cartesian grid that does not conform to the geometry of the elastic structure. The motion of the elastic structure will be described using Lagrangian variables defined on a curvilinear mesh. The IB method employs these two different grids and sets of variables that communicate with each other via the forcing term of the structure. This allows for a straightforward implementation of complicated fluid-structure interactions since the underlying Cartesian grid for the fluid domain is not required to coincide with the Lagrangian structure. With an evolving structure, the computational complexity is greatly reduced when a stationary, non-deforming Cartesian grid is used versus remeshing at each time step to have the structure conform to the fluid grid.

Let Ω be the fluid domain, which can be a subset of $\mathbb{R}^2$, a subset of $\mathbb{R}^3$, or an infinite fluid domain (all of $\mathbb{R}^2$ or $\mathbb{R}^3$). For this discussion, we will restrict Ω as a subset of $\mathbb{R}^2$. In Ω, points within the fluid that lie on the Cartesian grid of the fluid domain will be represented as $\mathbf{x}$, where $\mathbf{x} = (x_1, x_2)$ in 2-d. The velocity field $\mathbf{u}(\mathbf{x}, t)$ and pressure $p(\mathbf{x}, t)$ are Eulerian variables that are defined at each point on the Cartesian grid, corresponding to the fluid domain Ω. In the classical IB method, we assume the Newtonian fluid flow is governed by either the Navier-Stokes (NS) or Stokes (St) equation,

(2.1a)
$$\rho\left(\frac{\partial \mathbf{u}(\mathbf{x},t)}{\partial t} + \mathbf{u}(\mathbf{x},t)\cdot\nabla\mathbf{u}(\mathbf{x},t)\right) = -\nabla p(\mathbf{x},t) + \mu\nabla^2\mathbf{u}(\mathbf{x},t) + \mathbf{f}(\mathbf{x},t), \qquad \text{(NS)}$$

(2.1b)
$$0 = -\nabla p(\mathbf{x},t) + \mu\nabla^2\mathbf{u}(\mathbf{x},t) + \mathbf{f}(\mathbf{x},t), \qquad \text{(St)}$$

where $\mathbf{f}(\mathbf{x}, t)$ is the Eulerian force density on the Cartesian grid and μ and ρ are the constant fluid viscosity and density, respectively. Both fluids are assumed to be incompressible and therefore satisfy

(2.2)
$$\nabla\cdot\mathbf{u}(\mathbf{x},t) = 0 \ .$$

When Eq. (2.1a) is nondimensionalized, the Reynolds number $Re = \rho V L/\mu$ is a nondimensional ratio corresponding to the relative contributions of inertial forces to viscous forces where V is a characteristic velocity and L is a characteristic length.

The incompressible Stokes equations, given in Eqs. (2.1b) and (2.2), correspond to the case of zero Reynolds number, where viscous forces dominate and inertial forces can be neglected.

The structure is parameterized by s and we denote the position of the elastic structure at time t by $\mathbf{X}(s,t)$. In this simplified representation, one can model elastic structures corresponding to open or closed curves. We assume that the structure is neutrally buoyant and massless. The Lagrangian domain of the immersed structure is $\mathcal{B}$. The elastic structure exerts a Lagrangian force density on the surrounding fluid and is given by $\mathbf{F}(\mathbf{X},t)$. In order to determine the Eulerian force density $\mathbf{f}(\mathbf{x},t)$, we need to spread the Lagrangian force density $\mathbf{F}(\mathbf{X},t)$ to the Cartesian grid via the following interaction equation,

$$\mathbf{f}(\mathbf{x},t) = \int_{\mathcal{B}} \mathbf{F}(\mathbf{X},t)\delta_c(\mathbf{x}-\mathbf{X})ds, \tag{2.3}$$

where δ_c is a compactly supported smooth approximation to a δ distribution. This distributes the singular force layer $\mathbf{F}(\mathbf{X},t)$ to the surrounding fluid such that $\mathbf{f}(\mathbf{x},t)$ is mainly zero except in a small region around the structure. Examples of compactly supported delta functions and important properties are defined in §2.1.2 and a description of the derivation of a Lagrangian force density $\mathbf{F}(\mathbf{X},t)$ is given in §2.1.3.

The motion of the fluid is coupled to the motion of the elastic structure, thus we must also have a prescribed condition for the movement of the structure. Since the structure is immersed in a viscous fluid, the velocity across the structure will be continuous. Therefore, we can enforce a no-slip condition,

$$\frac{\partial \mathbf{X}}{\partial t} = \mathbf{U}(\mathbf{X},t) \tag{2.4a}$$

$$= \int_{\Omega} \mathbf{u}(\mathbf{x},t)\delta_c(\mathbf{x}-\mathbf{X})d\mathbf{x}, \tag{2.4b}$$

where the elastic structure $\mathbf{X}(s,t)$ will move with the local fluid velocity at that point, $\mathbf{U}(\mathbf{X},t)$. Since the fluid velocity is solved for on the Cartesian grid, we must use Eq. (2.4b) to interpolate the velocity $\mathbf{u}(\mathbf{x},t)$ to get the velocity at the immersed boundary points, $\mathbf{U}(\mathbf{X},t)$. Assuming we have the necessary boundary conditions for the fluid flow and/or pressure on Ω, we can solve the incompressible fluid equations, either Eq. (2.1a) or (2.1b) with Eq. (2.2), for a given immersed structure's force density $\mathbf{F}$ in Eq. (2.3) using a variety of methods including projection methods and the use of FFTs on periodic domains [**15**, **62**, **92**, **118**]. Sample results of the IB method are given in Fig. 1, where the forces on the immersed boundary points of the structure are proportional to curvature. The Lagrangian and Eulerian force density are shown in Fig. 1(a) and (b), respectively.

2.1.1. *Summary of Numerical Method.* To simplify, let the fluid domain Ω be a subset of $\mathbb{R}^2$ that is discretized into a uniform Cartesian grid with mesh width h such that $x_i = x_{i-1} + h$, $y_j = y_{j-1} + h$, and $\mathbf{x}_{ij} = (x_i, y_j)$ for $i = 1, \ldots, q$ and $j = 1, \ldots, r$. The structure $\mathbf{X} = (X_k, Y_k)$ will be discretized at time $t = 0$ to have uniform spacing for $k = 1, \ldots, m$ immersed boundary points. At time step n, assume we have a given discretized configuration of the structure $\mathbf{X}_k^n$. An outline of the numerical algorithm is as follows:

(1) Evaluate the problem dependent elastic Lagrangian force density $\mathbf{F}_k^n$ for the structure at each of the immersed boundary points $\mathbf{X}_k^n$

(2) Smooth the force density to the grid via Eq. (2.3) to determine the Cartesian grid force density $\mathbf{f}_{ij}^n$
(3) Solve the fluid equations, Eq. (2.1a) or (2.1b) using the incompressibility condition in Eq. (2.2) and the problem dependent fluid domain boundary conditions to determine $\mathbf{u}^{n+1}(\mathbf{x}_{ij})$ at each of the Cartesian grid points
(4) Interpolate the Cartesian grid velocity to the Lagrangian structure via Eq. (2.4b) to determine $\mathbf{U}^{n+1}(\mathbf{X}_k^n)$ at each of the immersed boundary points
(5) Update the location of the structure. Use Euler method or higher order methods such as Runge-Kutta methods to determine $\mathbf{X}^{n+1}$ using the no-slip condition given in Eq. (2.4a)
(6) Repeat

There are a few additional pieces of information to emphasize. In immersed boundary applications, if we have an elastic structure, we want to require that Δs is sufficiently small in order to ensure that fluid is not leaking across the immersed structure. It has been previously shown that this can be done if we choose $\Delta s = h/2$ [**138**]. In general, most numerical methods handle the force term explicitly, resulting in a severe time step restriction due to the stiff material properties of the immersed structure (see §3.1). Since the immersed boundary smooths or smears a sharp interface or singular force layer with a smooth approximation to the delta function, the interface then inherits a thickness that is equivalent to the mesh width. Above, we have assumed a uniform Cartesian grid where the Eulerian fluid and pressure are defined. Since the lowest accuracy is in the region of the immersed structure, adaptive grid methods have been developed to have finer detail in the region around the boundary to resolve boundary layers or regions of larger vorticity [**63**]. An explicit, formally second-order accurate in space and time numerical method, given sufficient smoothness (e.g. thicker boundaries), has been developed for the IB method using a projection-type method [**62**, **92**]. A convergence proof has been developed for a simplified immersed boundary problem of Stokes flow with an external force field supported on a curve [**123**]. Mori is able to give pointwise error estimates away from the immersed boundary as well as global L^∞ error estimate of the velocity. The work of Mori [**123**] was a major convergence result, proving that the velocity field solved for in the IB method converges to the true solution.

2.1.2. *Delta function.* The delta function δ_c in Eq. (2.3) and (2.4b) is replaced by a product of one-dimensional discrete delta functions that are scaled by the mesh width h. For example, in 3-d,

$$\delta_c(\mathbf{x}) = \frac{1}{h^3}\phi\left(\frac{x_i}{h}\right)\phi\left(\frac{y_j}{h}\right)\phi\left(\frac{z_k}{h}\right) \tag{2.5}$$

where h is mesh width. We note that spreading is the adjoint of interpolation when the same delta function is used in both Eqs. (2.3) and (2.4b) [**138**]. Now we will consider how to determine $\phi(r)$ satisfying certain properties, where r is defined as x_i/h, y_j/h, or z_k/h. The goal is to have a continuous ϕ in order to avoid jumps in velocity or force on the Cartesian grid. We wish to enforce, in a distributional sense, that $\delta_c \to \delta$ when $h \to 0$. To increase computational efficiency, we can require that $\phi(r)$ has compact support, e.g. $\phi(r) = 0$ for $r \geq 2$. In order to interpolate the velocity from the Cartesian grid to the Lagrangian structure in Eq. (2.4b), we wish to enforce exact interpolation of linear functions and second order interpolation for smooth functions. This can be satisfied if ϕ is chosen to satisfy the following

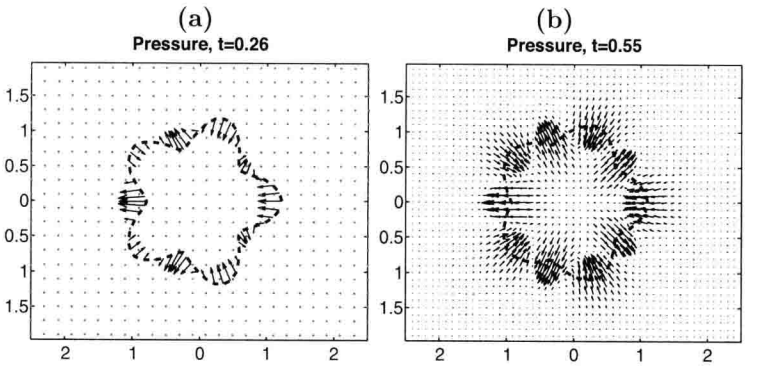

FIGURE 1. An example of an immersed boundary simulation where forces are proportional to the curvature. In (a), the perturbed circle is immersed in a viscous, incompressible fluid and visualized with the dashed lines. A subset of the Cartesian grid points are denoted by smaller circles on the domain and the Lagrangian singular force density $\mathbf{F}(\mathbf{X},t)$ on the immersed boundary are shown with the vectors on the structure. In (b), this is a later time point where the Eulerian force density $\mathbf{f}(\mathbf{X},t)$ is shown on the Cartesian grid by spreading the Lagrangian force density via Eq. (2.3).

equations,

$$\sum_{j\ even} \phi(r-j) = \sum_{j\ odd} \phi(r-j) = \frac{1}{2}\,, \tag{2.6a}$$

$$\sum_{j} (r-j)\phi(r-j) = 0\,, \tag{2.6b}$$

for all real r. The first equation, (2.6a), is an even-odd and zero$^{\text{th}}$ moment condition, which ensures that the central difference operators apply the correct weight to the points. The second equation, (2.6b), is a first moment condition. An example of a function ϕ that satisfies these conditions and others is,

$$\phi(r) = \begin{cases} 0 & |r| \geq 2 \\ \frac{1}{8}(5+2r-\sqrt{-7-12r-4r^2}), & -2 \leq r \leq -1 \\ \frac{1}{8}(3+2r+\sqrt{1-4r-4r^2}), & -1 \leq r \leq 0 \\ \frac{1}{8}(3-2r+\sqrt{1+4r-4r^2}), & 0 \leq r \leq 1 \\ \frac{1}{8}(5-2r-\sqrt{-7+12r-4r^2}), & 1 \leq r \leq 2 \end{cases}\,. \tag{2.7}$$

In order to have expressions for mass, momentum, and torque be the same when evaluated both in the Lagrangian and Eulerian form, this will depend on the specific properties of the delta function used [**138**]. Please refer to [**138**] for a list of additional conditions to determine the compactly supported delta function given in Eq. (2.7). Recently, Liu and Mori [**113**] have further analyzed properties of delta functions in reference to convergence of the IB method. They have shown that another property, called the smoothing order, is also very important in terms of convergence.

2.1.3. *Forces and Energy Functions.* The force density that the elastic structure exerts on the surrounding fluid will vary greatly based on the properties of the given structure. The stress and deformation of the elastic structure are determined by a given constitutive law and this is then transmitted to the fluid through a localized force density term in the momentum equations, either Eq. (2.1a) or (2.1b). To highlight a few basic principles, we will briefly describe a few types of force densities that may be included at a given point in time on the structure. Since the immersed structure is assumed to be neutrally buoyant, traditional IB methods do not account for gravitational forces.

A structure can be assigned a prescribed motion. This has been used to represent structures with zero or minimal movement as well as structures that have a time dependent prescribed motion [**8**, **39**, **92**]. In this formulation, we think of a stiff spring with a restoring force that attempts to keep the given point at the desired or 'tethered' configuration. The discretized form of this force density is,

$$\mathbf{F}_k = -\mathcal{S}_T(\mathbf{X}_k - \mathbf{X}_k^{tether}) \tag{2.8}$$

where $\mathcal{S}_T$ is a coefficient and $\mathbf{X}_k^{tether}$ is the tethered or desired location for the k^{th} immersed boundary point. We can view a tether force density as a spring with zero resting length connecting $\mathbf{X}_k^{tether}$ and $\mathbf{X}_k$. This tends to penalize deviations from the desired configuration.

In the IB method, the immersed structure is generally assumed to be elastic. In order to describe the stretching of this elastic structure, we idealize elastic links connecting the points via stiff springs that are assumed to be governed by Hooke's law (linear spring force). Between the points $\mathbf{X}_k$ and $\mathbf{X}_{k+1}$, the spring connecting these two points is generating force at each of these two points, trying to maintain the specified separation. This corresponds to the following discretized form of the force density $\mathbf{F}$ exerted on the surrounding fluid at the point $\mathbf{X}_k$,

$$\begin{aligned}\mathbf{F}(\mathbf{X}_k) = &-\left[\mathcal{S}_H\left(||\mathbf{X}_k - \mathbf{X}_{k-1}|| - \ell\right)\frac{\mathbf{X}_k - \mathbf{X}_{k-1}}{||\mathbf{X}_k - \mathbf{X}_{k-1}||}\right] \\ &-\left[\mathcal{S}_H\left(||\mathbf{X}_{k+1} - \mathbf{X}_k|| - \ell\right)\frac{\mathbf{X}_k - \mathbf{X}_{k+1}}{||\mathbf{X}_{k+1} - \mathbf{X}_k||}\right]\end{aligned} \tag{2.9}$$

where $\mathcal{S}_H$ is a spring constant or stiffness coefficient, $||\cdot||$ denotes the Euclidean norm, and ℓ is the resting spring length, which corresponds to the immersed boundary spacing in many problems. In Eq. 2.9, the first term corresponds to the spring force due to the spring connecting $\mathbf{X}_{k-1}$ and $\mathbf{X}_k$ and the second term corresponds to the spring force between $\mathbf{X}_k$ and $\mathbf{X}_{k+1}$. If a larger value of $\mathcal{S}_H$ is specified, this will cause the rest length to be more strictly enforced. We can also approximate inextensible materials by using a very large stiffness coefficient $\mathcal{S}_H$. We can also formulate the force in terms of the tension in a fiber or section of the immersed structure. The fiber is assumed to only sustain tension in the direction of the fiber, τ. Then, force balance on a given segment of the fiber can be used to write the force density as

$$\mathbf{F} = -\frac{\partial}{\partial s}(T\tau)\,, \tag{2.10a}$$

$$\tau = \frac{\frac{\partial \mathbf{X}}{\partial s}}{\left|\left|\frac{\partial \mathbf{X}}{\partial s}\right|\right|}\,, \tag{2.10b}$$

where τ is the unit tangent vector. When we assume the tension T on the fiber is a linear function of the fiber strain, we can write:

$$T = \mathcal{S}\left|\left|\frac{\partial \mathbf{X}}{\partial s}\right|\right| \tag{2.11}$$

where $\mathcal{S}$ is a stiffness coefficient. In this particular case, the force density becomes

$$\mathbf{F} = -\mathcal{S}\frac{\partial^2 \mathbf{X}}{\partial s^2}\,. \tag{2.12}$$

If a centered difference approximation of the derivative in Eq.(2.12) is used, one arrives at an expression like Eq. (2.9) for the force at a given point on the immersed structure. Thus, a spring model can be formulated as a discretization of the above fiber model.

We can also determine force density by first postulating an energy functional E that determines the elastic potential energy stored in the structure at a given time point. This postulated variational energy functional is set up to ensure that it is non-negative, translation and rotation invariant, and formulated such that the structure will want to minimize this energy. If we consider a perturbation of the given structure $\mathbf{X}$ as $\mathcal{P}\mathbf{X}$, the corresponding perturbation in the elastic energy is

$$\mathcal{P}E = -\int_{\mathcal{B}} (\mathbf{F}\cdot\mathcal{P}\mathbf{X}(s,t))ds\,, \tag{2.13a}$$

$$\mathbf{F} = -\frac{\mathcal{P}E}{\mathcal{P}\mathbf{X}}\,, \tag{2.13b}$$

where $\mathbf{F}$ is the Frechet derivative of E, defined implicity and corresponding to the amount of force that is generated by a perturbation in the elastic structure. Note that $\mathbf{F}$ corresponds to the force density exerted by the structure on the surrounding fluid and this formulation corresponds to virtual work on an elastic structure due to a perturbation of the structure.

In this energy formulation, the extent to which the energy is minimized will depend on the material properties of the elastic structure as well as the surrounding fluid environment. As an example, we could assume the following elastic energy (stretching),

$$E = \int_{\mathcal{B}} \mathcal{E}\left(\left|\left|\frac{\partial \mathbf{X}}{\partial s}\right|\right|\right) ds \tag{2.14}$$

where $\mathcal{E}$ is a local stretching energy density to be specified. This energy corresponds to the elasticity determined by the strain in the direction of the fiber, as derived above. Using this energy, the perturbation operator can be applied to both sides of Eq. (2.14). Assuming that tension T in Eq. (2.11) is also equivalent to the derivative of $\mathcal{E}'(||\partial\mathbf{X}/\partial s||)$, we can use integration by parts to simplify the integral. Thus, we can arrive at Eq. (2.12) or Eq. (2.9) using an energy argument. This energy formulation and derivation can also be extended to more complicated elastic structures.

For a more extensive derivation and examples, we refer the reader to [**138**]. Additionally, we wish to note that the choice of parameters in these energy functions and forces are not always determined in an ad hoc manner. For a given application, one can choose stiffness parameters to reflect the material properties of the structure. In order to estimate the flexural rigidity of an elastic structure, one can follow the procedure of Lim and Peskin [**108**].

2.2. Immersed interface method. The IB method is a powerful numerical method but as with almost all numerical methods, it has some drawbacks. IB methods are typically first-order accurate in the infinity norm. Also, because the boundary forces are spread out, the jump discontinuity in the pressure solution is not captured; instead, the computed pressure approximation has a sharp gradient near the immersed boundary. In fact, the pressure approximation has $\mathcal{O}(1)$ L_{inf} error and error in the pressure gradient translates into inaccuracy in boundary velocity. As a result, the IB method is known to exhibit "leakage" (i.e., an area in 2-d or a volume in 3-d enclosed by the immersed boundary or surface tends to decrease in time), unless corrective procedures are applied (e.g., [**32**, **136**]).

As a remedy, LeVeque and Li developed the immersed interface method, which yields second-order accurate approximates and robustly captures jump discontinuities in the solution and its derivatives. The key idea of the immersed interface method is to incorporate known jumps in the solution into the finite difference stencil. This method has been successfully implemented and used for both 2-d and 3-d fluids.

2.2.1. *A simple elliptic interface problem.* To motivate the immersed interface method, let's first consider a simple 1-d elliptic interface problem:

$$(\beta u_x)_x = f + \sigma\delta(x-\alpha), \quad 0 < x, \alpha < 1\,, \tag{2.15}$$

where f is smooth but β is discontinuous at $x = \alpha$. We re-state the problem in terms of the jump conditions:

$$(\beta u_x)_x = f, \quad x \in (0,\alpha) \cup (\alpha, 1), \tag{2.16}$$

$$[u] \equiv u^+ - u^- = 0, \quad [\beta u_x] = \sigma, \quad [\beta u_{xx}] = 0\,. \tag{2.17}$$

where $u^{\pm} \equiv \lim_{\epsilon \to 0^+} u(\alpha \pm \epsilon)$.

Suppose we discretize Eq. (2.16) using a centered difference scheme. We will separately consider grid points that are sufficiently far from $x = \alpha$ such that the associated finite difference stencils do not cross $x = \alpha$ (which will be referred to as "regular points"), and those whose stencils do cross $x = \alpha$ ("irregular"). For a regular point x_i, the discretized form of Eq. (2.16) is

$$\frac{1}{h^2}\left(\beta_{i+\frac{1}{2}}\left(u_{i+1} - u_i\right) - \beta_{i-\frac{1}{2}}\left(u_i - u_{i-1}\right)\right) = f_i \tag{2.18}$$

where h denotes the mesh width.

The finite stencil for an *irregular* point x_i, where $x_i < \alpha < x_{i+1}$, will need to be modified in order to attain second-order accuracy. Also, a correction term C_i will be added:

$$a u_{i-1} + b u_i + c u_{i+1} = f_i + C_i \tag{2.19}$$

To determine the coefficients and correction term C_i, we apply Taylor expansion of u_{i+1} and u_{i-1} around α:

$$u(x_{i+1}) = u^+(\alpha) + (x_{i+1} - \alpha)u_x^+(\alpha) + \frac{1}{2}(x_{i+1} - \alpha)^2 u_{xx}^+(\alpha) + \mathcal{O}(h^3) \tag{2.20}$$

$$u(x_{i-1}) = u^-(\alpha) + (x_i - \alpha)u_x^-(\alpha) + \frac{1}{2}(x_i - \alpha)^2 u_{xx}^-(\alpha) + \mathcal{O}(h^3) \tag{2.21}$$

Now recall that

$$[\beta u_x] = \sigma \Rightarrow \beta^+ u_x^+ - \beta^- u_x^- = \sigma$$

which, together with $u^+ = u^-$ and $u^+_{xx} = u^-_{xx}$, can be used to eliminate from Eq. (2.20) all u terms with right-side limits to yield

(2.22)
$$u(x_{i+1}) = u^-(\alpha) + (x_{i+1} - \alpha)\left(\frac{\beta^-}{\beta^+}u^-_x(\alpha) + \frac{\sigma}{\beta^+}\right) + \frac{1}{2}(x_{i+1} - \alpha)^2 u^-_{xx}(\alpha) + \mathcal{O}(h^3)$$

Substituting Eqs. (2.21) and (2.22) into Eq. (2.19) and rearranging, one obtains

$$\begin{aligned} &au_{i-1} + bu_i + cu_{i+1} \\ =&(a+b+c)u^-(\alpha) + \left((x_{i-1} - \alpha)a + (x_i - \alpha)b + \frac{\beta^-}{\beta^+}(x_{i+1} - \alpha)c\right)u^-_x(\alpha) \\ &+ c(x_{i+1} - \alpha)\frac{\sigma}{\beta^+} + \frac{1}{2}\left((x_{i-1} - \alpha)^2 a + (x_i - \alpha)^2 b + \frac{\beta^-}{\beta^+}(x_{i+1} - \alpha)^2 c\right)u^-_{xx}(\alpha) \\ =&(\beta u_x)_x = f_i + C_i \end{aligned}$$

By matching the coefficients in front of $u^-(\alpha)$, $u^-_x(\alpha)$, and $u^-_{xx}(\alpha)$, we obtain the following linear system

(2.23)
$$a + b + c = 0$$

(2.24)
$$\left((x_{i-1} - \alpha)a + (x_i - \alpha)b + \frac{\beta^-}{\beta^+}(x_{i+1} - \alpha)c\right)u^-_x(\alpha) = 0$$

(2.25)
$$\frac{1}{2}\left((x_{i-1} - \alpha)^2 a + (x_i - \alpha)^2 b + \frac{\beta^-}{\beta^+}(x_{i+1} - \alpha)^2 c\right) = \beta^-$$

which can be solved for a, b, and c. Then by equating the higher-order terms, we obtain an expression for the correction terms:

(2.26)
$$C_i = c(x_{i+1} - \alpha)\frac{\sigma}{\beta^+}$$

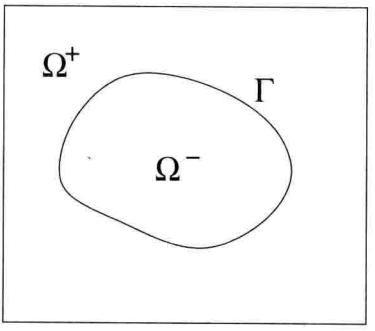

FIGURE 2. Model configuration for an immersed interface problem.

2.2.2. *Stokes and Navier-Stokes equations.* The singular boundary forces induce jump discontinuities in the pressure and normal derivatives of the velocity. But unlike the elliptic interface problem in the preceeding subsection, those jump conditions are not given explicitly. Instead, they can be computed from the boundary forces. Let f_n and f_τ denote the normal and tangential components of the

boundary forces, expressed per unit current arclength α, then it has been shown that for the Stokes equations [**100**]

$$[p] = f_n, \quad [p_n] = \frac{\partial}{\partial \alpha} f_\tau, \tag{2.27}$$

$$[u] = [v] = 0, \tag{2.28}$$

$$[\mu u_n] = f_\tau \sin\theta, \quad [\mu v_n] = -f_\tau \cos\theta \tag{2.29}$$

where θ denotes the angle between the tangent line and the x-axis. Model configuration for a immersed interface problem is illustrated in Fig. 2. Note that the immersed boundary is a closed curve. This is no accident. The derivative of the jump conditions (2.27)–(2.29) requires a closed curve (or closed surface in 3-d). This is indeed a limitation of the immersed interface method that the IB method does not share.

We will describe the procedures by which the steady-state Stokes equations can be solved using the immersed interface method. The immersed interface method can also be applied to the Navier-Stokes equations [**103, 169**], but as might be expected, the procedures are more complicated. For a fluid with uniform viscosity, the Stokes equations are (2.1b) and (2.2); that system can be solved simultaneously as a coupled system. Alternatively, the system can be reduced to a sequence of three Poisson problems, as described below. Applying the divergence operator to Eq. (2.1b) yields

$$\Delta p = \nabla \cdot \mathbf{f} \tag{2.30}$$

which we will solve by setting the right-hand-side to zero and by incorporating the jump conditions (2.27). Consider the 2-d problem following a procedure similar to §2.2.1, we discretize Eq. (2.30) to obtain the finite-difference equations

$$\frac{1}{h^2}\left(p_{i+1,j} + p_{i-1,j} - 4p_{i,j} + p_{i,j-1} + p_{i,j+1}\right) = C_{i,j} \tag{2.31}$$

where the correction terms $C_{i,j}$ are zero except at irregular points.

Next we solve the Poisson equations (2.1b) for u and v. The finite difference equation for u takes the form

$$\frac{1}{h^2}\left(u_{i+1,j} + u_{i-1,j} - 4u_{i,j} + u_{i,j-1} + u_{i,j+1}\right) = \frac{1}{2h\mu}\left(p_{xi+1,j} - p_{xi-1,j}\right) + \hat{C}_{i,j} \tag{2.32}$$

where the correction term $\hat{C}_{i,j}$ corrects for the approximation of p_x, and accounts for the jump discontinuities in the derivative of u. The procedure for v is analogous.

To summarize, the steps in which the immersed interface method can be used to simulate the interactions between a Stokes fluid and an immersed boundary are as follows. At time t^n, the boundary position $\mathbf{X}^n$ is known.

(1) From the boundary configuration $\mathbf{X}^n$, compute boundary forces $\mathbf{f}^n$.
(2) From the boundary forces $\mathbf{f}^n$, compute jump conditions (2.27)–(2.29).
(3) Form the correction terms, which are functions of the jump conditions above, and solve Eqs. (2.31) and (2.32), plus analogous equation for v.
(4) Advance the boundary (see §2.1).

2.3. Regularized Stokeslet method. Many fluid-structure interaction problems involve small length scales and/or large viscosity, where the Reynolds number is approximately zero. In these applications, one could use the IB method detailed

in §2.1, solving the incompresible Stokes equations in Eq. (2.1b)-(2.2) or solving the incompressible Navier-Stokes equations with $Re \approx 10^{-4} - 10^{-6}$ in Eq. (2.1a) and (2.2). In the case of zero Reynolds number applications, other methods can be used since the Stokes equations are linear, have no memory, and the only time dependence will be from a forcing term due to the immersed structure. Fundamental solutions exist for the Stokes equations; this allows for the use of Lagrangian methods such as boundary integral methods and the method of regularized Stokeslets as an alternative to the IB method.

In a 2-d infinite fluid domain, the Stokeslet (or Green's function) is the fluid flow that results from a point force of strength $\mathbf{g}_o$ applied at the point $\mathbf{X}_o$ and is given by

$$\mathbf{u}_s(\mathbf{x}) = \frac{-\mathbf{g}_o}{4\pi\mu}\ln(r) + \frac{[\mathbf{g}_o \cdot (\mathbf{x}-\mathbf{X}_o)](\mathbf{x}-\mathbf{X}_o)}{4\pi\mu r^2} \quad \text{(2-d)} \tag{2.33}$$

where $r = ||\mathbf{x} - \mathbf{X}_o||$. The velocity behaves like $\ln(r)$ in the 2-d Stokeslet. We will primarily focus this discussion on 2-d fluids. However, there is also a fundamental solution for a point force in a 3-d fluid that behaves like $1/r$.

The structures can be closed or open curves, as well as sets of disconnected points. The forces are then applied on the given structure. Due to the linearity of the Stokes equation, we can write the resulting velocity as a superposition of Stokeslets when there are several point forces. The method of regularized Stokeslets, developed by Cortez *et al.* [**29**, **31**], regularizes the singularity at $\mathbf{x} = \mathbf{X}_o$ in the denominator. The approach is similar to that of the IB method, in that the singular force will be spread to the surrounding fluid.

In the IB method, a compactly supported smooth approximation to the δ function was used to spread forces to the Cartesian fluid grid via Eq. (2.3). Here, we will use a blob or cutoff function ψ_ϵ that is a radially symmetric approximation to the δ function. The cutoff function can have compact or infinite support and has that the property that the integral of ψ_ϵ on the infinite fluid domain is equal to 1. Note that since this a Lagrangian method, an infinite support blob does not decrease computational efficiency as it would in the standard IB method introduced in §2.1. If using a blob function with infinite support, the majority of the force will be concentrated within a region around the point force and will then decay quickly. An example blob function is,

$$\psi_\epsilon = \frac{2\epsilon^4}{\pi(r^2+\epsilon^2)^3} \quad \text{(2-d)}. \tag{2.34}$$

The form of the blob functions are derived in order to solve Stokes equations for a regularized force as well as ensuring that when taking $\lim \epsilon \to 0$, we recover a δ function.

In the method of regularized Stokeslets (MRS), we wish to solve the incompressible Stokes equations where the force density $\mathbf{f}$ is given as a regularized point force $\mathbf{g}_o$ at $\mathbf{X}_o$,

$$\mu\Delta\mathbf{u}(\mathbf{x}) = \nabla p(\mathbf{x}) - \mathbf{g}_o\psi_\epsilon(\mathbf{x}-\mathbf{X}_o) \ , \tag{2.35a}$$

$$\nabla \cdot \mathbf{u}(\mathbf{x}) = 0 \ . \tag{2.35b}$$

The exact solution is no longer the Stokeslet as given in Eq. (2.33). For a given choice of regularization function ψ_ϵ, we now need to derive a regularized Green's function G_ϵ that satisfies $\Delta G_\epsilon = \psi_\epsilon$. Since ψ_ϵ is radially symmetric, we assume